Coherent superconducting qubits from a subtractive junction fabrication process

Alexander Stehli,[1,a)] Jan David Brehm,[1] Tim Wolz,[1] Paul Baity,[2] Sergey Danilin,[2] Valentino Seferai,[2] Hannes Rotzinger,[1,3] Alexey V. Ustinov,[1,4,5] and Martin Weides[2]

[1)]*Institute of Physics, Karlsruhe Institute of Technology, 76131 Karlsruhe, Germany*

[2)]*James Watt School of Engineering, University of Glasgow, Glasgow G12 8LT, United Kingdom*

[3)]*Institute for Quantum Materials and Technologies, Karlsruhe Institute of Technology, 76344 Eggenstein-Leopoldshafen, Germany*

[4)]*National University of Science and Technology MISIS, Moscow 119049, Russia*

[5)]*Russian Quantum Center, Skolkovo, Moscow 143025, Russia*

(Dated: 8 September 2020)

Josephson tunnel junctions are the centerpiece of almost any superconducting electronic circuit, including qubits. Typically, the junctions for qubits are fabricated using shadow evaporation techniques to reduce dielectric loss contributions from the superconducting film interfaces. In recent years, however, sub-micron scale overlap junctions have started to attract attention. Compared to shadow mask techniques, neither an angle dependent deposition nor free-standing bridges or overlaps are needed, which are significant limitations for wafer-scale processing. This comes at the cost of breaking the vacuum during fabrication, but simplifies integration in multi-layered circuits, implementation of vastly different junction sizes, and enables fabrication on a larger scale in an industrially-standardized process. In this work, we demonstrate the feasibility of a subtractive process for fabrication of overlap junctions. In an array of test contacts, we find low aging of the average normal state resistance of only 1.6% over 6 months. We evaluate the coherence properties of the junctions by employing them in superconducting transmon qubits. In time domain experiments, we find that both, the qubit life- and coherence time of our best device, are on average greater than 20 µs. Finally, we discuss potential improvements to our technique. This work paves the way towards a more standardized process flow with advanced materials and growth processes, and constitutes an important step for large scale fabrication of superconducting quantum circuits.

Superconducting qubits are one of the most promising platforms to realize a universal quantum computer. In contrast to other popular qubit implementations, such as trapped ions[1], cold atoms[2], and NV centers[3], the properties of superconducting qubits are defined by a micro-fabricated electrical circuit. Consequently, most qubit parameters are adjustable by the circuit design and fabrication, and even the physical encoding of a quantum state is flexible[4–8]. Superconducting qubits feature good coherence times in the range of $10-300\,\mu s$[9–12], which is long enough for several hundred to thousand qubit gates[13]. Most recently, quantum advantage was for the first time demonstrated on a processor consisting of superconducting transmon qubits with an average lifetime of $T_1 = 16\,\mu s$[14].

The centerpiece of most superconducting qubits are Josephson junctions (JJ) serving as nonlinear elements. Their nonlinearity allows for the isolation of two of the circuit's quantum levels, usually ground, and first excited state, which may then be used as logical quantum states for computation. Currently, several different techniques are employed to generate the superconductor-insulator-superconductor interface of the JJ. Most processes rely on electron-beam lithography as smaller areas enable lower loss in the JJ[15,16]. In the commonly used shadow-evaporation processes, free standing bridges[17] or overhangs[18], and multi-angle evaporation are exploited to generate the desired interface in situ. One drawback of these techniques is a systematic angle dependent parameter spread across larger wafers, where great efforts are necessary to mitigate this spread[19,20]. The need for point-like evaporation sources limits the applicable materials and growth processes. When polymer masks are employed in favor of hard masks[21,22] the superconductor choice is further restricted to metals with low melting temperatures. Additionally, the JJ can suffer from an outgasing of the resist. An alternative to shadow-mask technology are overlap JJ, which do not rely on angle dependent evaporation, and therefore promise superior scalability. Early implementations of micron sized overlap JJ with superconducting qubits suffered significantly from dielectric loss[23–25]. More recently, qubits with nanoscaled contacts feature coherence properties competitive with those stemming from shadow-evaporation techniques[26].

However, current fabrication processes still rely on double resist stacks, and lift-off steps, limiting processing yield and presenting a potential source of contamination during the deposition[27,28].

In this work, we implement a subtractive process for patterning the JJ, where both electrodes are structured using etching rather than lift-off, allowing for smaller, more coherent contacts. Eliminating the resist from the evaporation chamber opens the door to homogeneous deposition, the addition of reactive gases, and evaporation at elevated temperatures. Consequently, new electrode materials, or epitaxial growth can be explored[29]. We demonstrate our fabrication platform using Al-AlO_x-Al JJ. Using an array of test contacts, we study aging of the room temperature resistance, which on average increases by only by 1.6% over 6 months. Transmon

a)corresponding author: alexander.stehli@kit.edu

qubits fabricated with this technique show good coherence properties, where the life-, and coherence times of our best device exceed on average 20 µs. The process is fully compatible with modern nanofabrication methods, making it an important ingredient for large scale fabrication of superconducting quantum processors.

A schematic of the fabrication process is displayed in Fig. 1a. In the first step, a c-plane sapphire wafer is covered with aluminum at a thickness of 50 nm, evaporated at a rate of 1 nm/s. This layer defines the main structures of the circuit, as well as the bottom electrode of the JJ. Following, the latter is patterned using electron-beam lithography with $\sim$ 180 nm thick PMMA resist. However, any resist with sufficient resistance to the etching plasma and a satisfactory resolution may be employed. A positive resist reduces electron-beam writing times. Subsequently, the structures are transferred to the aluminum film by reactive ion etching with an Ar/Cl plasma. The plasma is generated inductively using an rf-field with 100 W at a gas flow of 15 cm^3/min (sccm) argon and 2 sccm chlorine gas, and is accelerated with a power of 100 W. After etching, the remaining resist is removed with a combination of ultrasonic cleaning, acetone, and N-ethyl-pyrrolidone. Milling, oxidation, and deposition of the top electrode are performed in situ, in a Plassys™ MEB550S evaporation machine. First, resist residuals are incinerated in a 30 second Ar/O plasma. The native oxide on the aluminum film is removed by Ar sputtering for 180 seconds[30]. Immediately afterwards, the AlO_x tunnel barrier is grown in a controlled manner by dynamic oxidation for 30 minutes, admitting a continuous flow of 12 sccm O_2 to the load lock, at chamber pressure of $p_{\mathrm{LL}} \approx 0.195$ mbar. The 80 nm thick aluminum top layer is deposited in vacuum at a rate of 1 nm/s. Analogously to the bottom electrode, the top layer is patterned with electron-beam lithography and an Ar/Cl plasma. Finally, larger structures can be applied using optical lithography. We note, that this process leaves us with a stray junction, which was shown to have a negative impact on qubit coherence times[31]. This effect can be mitigated by employing a bandaging technique, which shorts the dielectric of the stray junction[32].

Using SEM imaging, we identify a process bias of $\sim 10\%$ towards reduced junction edge width. Most likely, the chlorine introduces an isotropic component of the etching plasma, causing an under-etching and sloped side-walls of the aluminum films, thus reducing the width of the contact electrodes. In room temperature measurements, we find a normal state resistance times area product of $R_nA = (0.47 \pm 0.10)\,\Omega\,\mu\mathrm{m}^2$ across 36 test contacts with varied size, fabricated in the same batch as our qubits. After aging for ~ 6 months this value increased by about 1.6%, see Fig. 2. This indicates clean JJ interfaces[27]. For additional information see supplementary material. The spread in resistance is similar to that found in shadow evaporated junctions (before meticulous process optimization). It is likely to be caused by the nonuniformity of the electrode edges, constituting $\sim 25-40\%$ of the total JJ area, due to an isotropic etching component caused by the chlorine. In the future, the spread in normal state resistance can be mitigated by reducing the thickness of both top and bottom electrode, and thereby the duration of the dry etch and effects of under-etching. This also enables the use of thinner electron-beam resists with better resolution. In combination, this allows to decrease overlap area, a crucial step for reducing dielectric loss in the JJ.

TABLE I. Device parameters in MHz. For each qubit, this includes the frequency of the readout resonator ω_{r}, and the first qubit transition ω_{01}, as well as the qubit anharmonicity α, the coupling strength g to the readout resonator, and the resulting disperive shift χ.

device	$\omega_{\mathrm{r}}/2\pi$	$\omega_{01}/2\pi$	$\alpha/2\pi$	$\chi_{01}/2\pi$	$g/2\pi$
q_1	6460	3548	−257	0.915	47.5
q_2	6632	3950	−262	0.514	45.6
q_3	6462	3161	−294	0.350	50.6
q_4	6457	3324	−300	0.774	49.3

Using the recipe described above, we fabricate a sample comprising two conventional (devices q_1 and q_2), and two concentric transmon qubits[33] (devices q_3 and q_4), embedded in a coplanar microwave environment, see Fig. 1b. A micrograph of the whole chip, our approach in identifying the qubits, and details on the qubit fabrication can be found in the supplementary material. For readout purposes, the qubits are capacitively coupled to a distributed $\lambda/4$-resonator, which are addressed in reflection measurements. The qubit population is determined by the dispersive shift of the respective readout resonator's frequency[34,35]. Table I summarizes the essential parameters of all four devices, which were extracted using spectroscopy measurements. The qubit-resonator coupling was calculated from the dispersive shift of the corresponding readout resonator.

We measure the lifetime T_1, Ramsey decay time T_2^{R}, and spin-echo decay time T_2 of all qubits over several hours. By employing an interleaved measurement scheme, we resolve slow fluctuations of the qubit frequencies, life-, and coherence times[36–38]. For each qubit, the combined measurement of a set of T_1, T_2^{R} and T_2 takes ~ 30 s for 10^3 point averages. A typical measurement trace from device q_4 is displayed in Fig. 3. Here, the $\pi/2$-pulse in the Ramsey-sequence was detuned by ~ 50 kHz, which results in characteristic oscillations in the laboratory frame of reference. For a detailed sketch of the measurement setup, see supplementary material.

A comparison of the coherence properties of all four qubits is displayed in Fig. 4, in a boxplot. For the full distribution we refer to the supplementary material. Data sets with a fit error exceeding 50% are neglected. Furthermore, we exclude traces where either of the coherence times exceeds $2T_1$, or where $T_2^{\mathrm{R}} > T_2$. The median lifetime $\tilde{T}_1$, coherence time $\tilde{T}_2^{\mathrm{R}}$, and $\tilde{T}_2$ of all four devices are summarized in table II.

Devices q_1-q_3 perform slightly worse than q_4. A potential cause is aluminum residuals in the vicinity of the JJ. The performance of device q_4 is close to the results of qubits with JJ made from shadow evaporation or lifted overlaps, with state of the art transmon qubits performing better by a factor of $\sim 5-10$. Here, our devices would profit from a reduction of surface loss[39], and optimization of the electrode

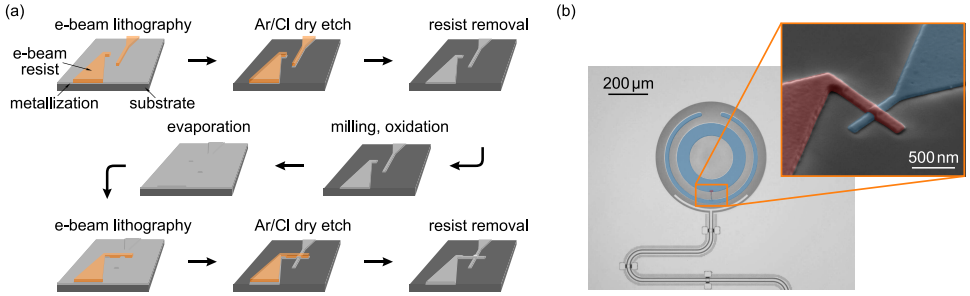

FIG. 1. a) Sketch of the fabrication process. The process solely relies on two etching steps to pattern the electrodes of the JJ. The lithography for the top layer is performed identically to that of the bottom electode. b) False color image of the concentric transmon qubit, and SEM micrograph of the JJ. The bottom layer of aluminum is highlighted in blue. The top layer, forming the second JJ electode, is colored in red. The JJ electrodes have a width of $\sim$ 180nm.

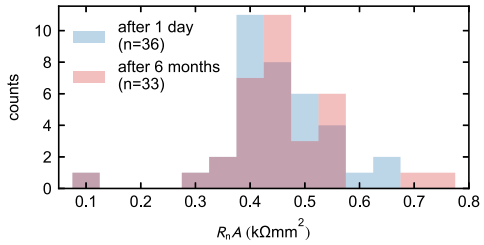

FIG. 2. Room temperature resistance measurements of the test JJ, before, and after aging. The resistance is normalized to the JJ area. We vary the latter by increasing the JJ edge width from 150 nm to 300 nm in 50 nm increments. The mean of R_nA increased by only 1.6% after $\sim$ 6 months of aging in ambient conditions.

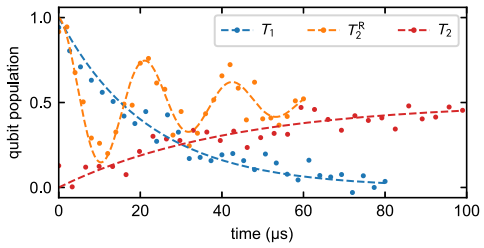

FIG. 3. Qubit population during a typical decay time measurement. The dashed lines represent a fit to the qubit's lifetime $T_1 = (22.0 \pm 0.9)\,\mu s$, and coherence times $T_2^R = (30.1 \pm 3.7)\,\mu s$ (Ramsey experiment) and $T_2 = (42.3 \pm 2.9)\,\mu s$ (spin-echo experiment).

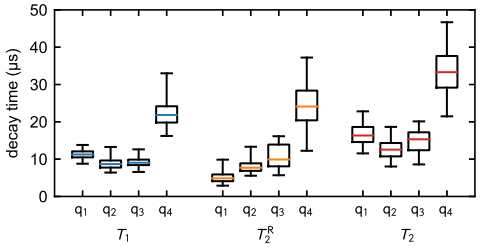

FIG. 4. Long-term measurement of the qubits' decay times. The box encloses the second and third quartile, whereas the whiskers indicate 2σ, i.e., 95% of the data. The colored line indicates the median of each data set.

TABLE II. Overview of the qubits' median lifetime $\tilde{T}_1$, and median coherence times $\tilde{T}_2^R$, and $\tilde{T}_2$ in µs.

device	$\tilde{T}_1$	$\tilde{T}_2^R$	$\tilde{T}_2$
q_1	11.3	4.9	16.3
q_2	8.7	7.7	12.5
q_3	9.0	9.9	15.3
q_4	21.8	24.1	33.3

materials[12].

In conclusion, we established a technique for the subtractive fabrication of coherent JJ. Our recipe does generally not rely on lift-off processes, is angle independent, and tolerates depositions at elevated temperatures and in reactive gases. Furthermore, our approach is extremely flexible with respect to the electrode materials, and growth processes. The junctions feature low aging of the normal state resistance, indicating clean JJ interfaces. These are important ingredients for streamlined and large scale processing platform of superconducting quantum processors. We demonstrated good

coherence properties of four transmon qubits with subtractive JJ, where the average life- and coherence times of our best device exceed 20 µs.

ACKNOWLEDGMENTS

Cleanroom facilities use was supported by the KIT Nanostructure Service Laboratory (NSL). We thank A. Lukashenko for technical support. This work was supported by the European Research Council (ERC) under the Grant Agreement No. 648011, Deutsche Forschungsgemeinschaft (DFG) projects INST 121384/138-1FUGG and WE 4359-7, EPSRC Hub in Quantum Computing and Simulation EP/T001062/1, and the Initiative and Networking Fund of the Helmholtz Association. AS acknowledges support from the Landesgraduiertenförderung Baden-Württemberg (LGF), JDB acknowledges support from the Studienstiftung des Deutschen Volkes. TW acknowledges support from the Helmholtz International Research School for Teratronics (HIRST). AVU acknowledges partial support from the Ministry of Education and Science of the Russian Federation in the framework of the Increase Competitiveness Program of the National University of Science and Technology MISIS (contract No. K2-2020-017).

DATA AVAILABILITY

The data that support the findings of this study are available from the corresponding author upon reasonable request.

SUPPLEMENTARY MATERIAL

See supplementary material for a description of the microwave setup, details on the qubit fabrication, additional information on room temperature measurements and JJ aging, the readout resonator identification, and the distributions of life- and coherence times of each qubit.

REFERENCES

[1] J. I. Cirac and P. Zoller, "Quantum Computations with Cold Trapped Ions," Physical Review Letters **74**, 4091–4094 (1995).
[2] I. Bloch, "Quantum coherence and entanglement with ultracold atoms in optical lattices," Nature **453**, 1016–1022 (2008).
[3] "Single defect centres in diamond: A review," physica status solidi (a) **203**, 3207–3225 (2006).
[4] Y. Nakamura, Y. A. Pashkin, and J. S. Tsai, "Coherent control of macroscopic quantum states in a single-Cooper-pair box," Nature **398**, 786–788 (1999).
[5] J. M. Martinis, S. Nam, J. Aumentado, and C. Urbina, "Rabi Oscillations in a Large Josephson-Junction Qubit," Physical Review Letters **89**, 117901 (2002).
[6] I. Chiorescu, Y. Nakamura, C. J. P. M. Harmans, and J. E. Mooij, "Coherent Quantum Dynamics of a Superconducting Flux Qubit," Science **299**, 1869–1871 (2003).
[7] J. Koch, T. M. Yu, J. Gambetta, A. A. Houck, D. I. Schuster, J. Majer, A. Blais, M. H. Devoret, S. M. Girvin, and R. J. Schoelkopf, "Charge-insensitive qubit design derived from the Cooper pair box," Physical Review A - Atomic, Molecular, and Optical Physics **76**, 42319 (2007).
[8] V. E. Manucharyan, J. Koch, L. I. Glazman, and M. H. Devoret, "Fluxonium: Single Cooper-Pair Circuit Free of Charge Offsets," Science **326**, 113–116 (2009).
[9] H. Paik, D. I. Schuster, L. S. Bishop, G. Kirchmair, G. Catelani, A. P. Sears, B. R. Johnson, M. J. Reagor, L. Frunzio, L. I. Glazman, S. M. Girvin, M. H. Devoret, and R. J. Schoelkopf, "Observation of high coherence in Josephson junction qubits measured in a three-dimensional circuit QED architecture," Physical Review Letters **107**, 240501 (2011).
[10] R. Barends, J. Kelly, A. Megrant, D. Sank, E. Jeffrey, Y. Chen, Y. Yin, B. Chiaro, J. Mutus, C. Neill, P. O'Malley, P. Roushan, J. Wenner, T. C. White, A. N. Cleland, and J. M. Martinis, "Coherent josephson qubit suitable for scalable quantum integrated circuits," Physical Review Letters **111**, 1–5 (2013).
[11] A. Nersisyan, E. A. Sete, S. Stanwyck, A. Bestwick, M. Reagor, S. Poletto, N. Alidoust, R. Manenti, R. Renzas, C.-V. Bui, K. Vu, T. Whyland, and Y. Mohan, "Manufacturing low dissipation superconducting quantum processors," in *2019 IEEE International Electron Devices Meeting (IEDM)*, Vol. 2019-Decem (IEEE, 2019) pp. 31.1.1–31.1.4.
[12] A. P. M. Place, L. V. H. Rodgers, P. Mundada, B. M. Smitham, M. Fitzpatrick, Z. Leng, A. Premkumar, J. Bryon, S. Sussman, G. Cheng, T. Madhavan, H. K. Babla, B. Jaeck, A. Gyenis, N. Yao, R. J. Cava, N. P. de Leon, and A. A. Houck, "New material platform for superconducting transmon qubits with coherence times exceeding 0.3 milliseconds," (2020), arXiv:2003.00024.
[13] M. Kjaergaard, M. E. Schwartz, J. Braumüller, P. Krantz, J. I.-J. Wang, S. Gustavsson, and W. D. Oliver, "Superconducting Qubits: Current State of Play," Annual Review of Condensed Matter Physics **11**, 369–395 (2020).
[14] F. Arute, K. Arya, R. Babbush, D. Bacon, J. C. Bardin, R. Barends, R. Biswas, S. Boixo, F. G. Brandao, D. A. Buell, B. Burkett, Y. Chen, Z. Chen, B. Chiaro, R. Collins, W. Courtney, A. Dunsworth, E. Farhi, B. Foxen, A. Fowler, C. Gidney, M. Giustina, R. Graff, K. Guerin, S. Habegger, M. P. Harrigan, M. J. Hartmann, A. Ho, M. Hoffmann, T. Huang, T. S. Humble, S. V. Isakov, E. Jeffrey, Z. Jiang, D. Kafri, K. Kechedzhi, J. Kelly, P. V. Klimov, S. Knysh, A. Korotkov, F. Kostritsa, D. Landhuis, M. Lindmark, E. Lucero, D. Lyakh, S. Mandrà, J. R. McClean, M. McEwen, A. Megrant, X. Mi, K. Michielsen, M. Mohseni, J. Mutus, O. Naaman, M. Neeley, C. Neill, M. Y. Niu, E. Ostby, A. Petukhov, J. C. Platt, C. Quintana, E. G. Rieffel, P. Roushan, N. C. Rubin, D. Sank, K. J. Satzinger, V. Smelyanskiy, K. J. Sung, M. D. Trevithick, A. Vainsencher, B. Villalonga, T. White, Z. J. Yao, P. Yeh, A. Zalcman, H. Neven, and J. M. Martinis, "Quantum supremacy using a programmable superconducting processor," Nature **574**, 505–510 (2019).
[15] J. M. Martinis, K. B. Cooper, R. McDermott, M. Steffen, M. Ansmann, K. D. Osborn, K. Cicak, S. Oh, D. P. Pappas, R. W. Simmonds, and C. C. Yu, "Decoherence in Josephson Qubits from Dielectric Loss," Physical Review Letters **95**, 210503 (2005).
[16] M. Weides, R. C. Bialczak, M. Lenander, E. Lucero, M. Mariantoni, M. Neeley, A. D. O'Connell, D. Sank, H. Wang, J. Wenner, T. Yamamoto, Y. Yin, A. N. Cleland, and J. Martinis, "Phase qubits fabricated with trilayer junctions," Superconductor Science and Technology **24**, 055005 (2011).
[17] G. J. Dolan, "Offset masks for lift-off photoprocessing," Applied Physics Letters **31**, 337–339 (1977).
[18] F. Lecocq, I. M. Pop, Z. Peng, I. Matei, T. Crozes, T. Fournier, C. Naud, W. Guichard, and O. Buisson, "Junction fabrication by shadow evaporation without a suspended bridge," Nanotechnology **22**, 315302 (2011).
[19] N. Foroozani, C. Hobbs, C. C. Hung, S. Olson, D. Ashworth, E. Holland, M. Malloy, P. Kearney, B. O'Brien, B. Bunday, D. DiPaola, W. Advocate, T. Murray, P. Hansen, S. Novak, S. Bennett, M. Rodgers, B. Baker-O'Neal, B. Sapp, E. Barth, J. Hedrick, R. Goldblatt, S. S. P. Rao, and K. D. Osborn, "Development of transmon qubits solely from optical lithography on 300 mm wafers," Quantum Science and Technology **4**, 025012 (2019).
[20] J. M. Kreikebaum, K. P. O'Brien, A. Morvan, and I. Siddiqi, "Improving wafer-scale Josephson junction resistance variation in superconducting quantum coherent circuits," Superconductor Science and Technology **33**, 06LT02 (2020).

[21] R. Dolata, H. Scherer, A. B. Zorin, and J. Niemeyer, "Single electron transistors with Nb/AlO[sub x]/Nb junctions," Journal of Vacuum Science & Technology B: Microelectronics and Nanometer Structures **21**, 775 (2003).
[22] I. Tsioutsios, K. Serniak, S. Diamond, V. V. Sivak, Z. Wang, S. Shankar, L. Frunzio, R. J. Schoelkopf, and M. H. Devoret, "Free-standing silicon shadow masks for transmon qubit fabrication," AIP Advances **10**, 065120 (2020).
[23] M. Steffen, M. Ansmann, R. McDermott, N. Katz, R. C. Bialczak, E. Lucero, M. Neeley, E. M. Weig, A. N. Cleland, and J. M. Martinis, "State Tomography of Capacitively Shunted Phase Qubits with High Fidelity," Physical Review Letters **97**, 050502 (2006).
[24] M. P. Weides, J. S. Kline, M. R. Vissers, M. O. Sandberg, D. S. Wisbey, B. R. Johnson, T. A. Ohki, and D. P. Pappas, "Coherence in a transmon qubit with epitaxial tunnel junctions," Applied Physics Letters **99**, 262502 (2011).
[25] J. Braumüller, J. Cramer, S. Schlör, H. Rotzinger, L. Radtke, A. Lukashenko, P. Yang, S. T. Skacel, S. Probst, M. Marthaler, L. Guo, A. V. Ustinov, and M. Weides, "Multiphoton dressing of an anharmonic superconducting many-level quantum circuit," Physical Review B **91**, 54523 (2015).
[26] X. Wu, J. L. Long, H. S. Ku, R. E. Lake, M. Bal, and D. P. Pappas, "Overlap junctions for high coherence superconducting qubits," Applied Physics Letters **111**, 032602 (2017).
[27] I. M. Pop, T. Fournier, T. Crozes, F. Lecocq, I. Matei, B. Pannetier, O. Buisson, and W. Guichard, "Fabrication of stable and reproducible submicron tunnel junctions," Journal of Vacuum Science & Technology B, Nanotechnology and Microelectronics: Materials, Processing, Measurement, and Phenomena **30**, 010607 (2012).
[28] C. M. Quintana, A. Megrant, Z. Chen, A. Dunsworth, B. Chiaro, R. Barends, B. Campbell, Y. Chen, I.-C. Hoi, E. Jeffrey, J. Kelly, J. Y. Mutus, P. J. J. O'Malley, C. Neill, P. Roushan, D. Sank, A. Vainsencher, J. Wenner, T. C. White, A. N. Cleland, and J. M. Martinis, "Characterization and reduction of microfabrication-induced decoherence in superconducting quantum circuits," Applied Physics Letters **105**, 062601 (2014).
[29] S. Fritz, L. Radtke, R. Schneider, M. Luysberg, M. Weides, and D. Gerthsen, "Structural and nanochemical properties of AlOx layers in Al-AlOx-Al-layer systems for Josephson junctions," Physical Review Materials **3**, 114805 (2019).
[30] L. Grünhaupt, U. Von Lüpke, D. Gusenkova, S. T. Skacel, N. Maleeva, S. Schlör, A. Bilmes, H. Rotzinger, A. V. Ustinov, M. Weides, and I. M. Pop, "An argon ion beam milling process for native AlOx layers enabling coherent superconducting contacts," Applied Physics Letters **111**, 072601 (2017).
[31] J. Lisenfeld, A. Bilmes, A. Megrant, R. Barends, J. Kelly, P. Klimov, G. Weiss, J. M. Martinis, and A. V. Ustinov, "Electric field spectroscopy of material defects in transmon qubits," npj Quantum Information **5**, 105 (2019).
[32] A. Dunsworth, A. Megrant, C. Quintana, Z. Chen, R. Barends, B. Burkett, B. Foxen, Y. Chen, B. Chiaro, A. Fowler, R. Graff, E. Jeffrey, J. Kelly, E. Lucero, J. Y. Mutus, M. Neeley, C. Neill, P. Roushan, D. Sank, A. Vainsencher, J. Wenner, T. C. White, and J. M. Martinis, "Characterization and reduction of capacitive loss induced by sub-micron Josephson junction fabrication in superconducting qubits," Applied Physics Letters **111**, 022601 (2017).
[33] J. Braumüller, M. Sandberg, M. R. Vissers, A. Schneider, S. Schlör, L. Grünhaupt, H. Rotzinger, M. Marthaler, A. Lukashenko, A. Dieter, A. V. Ustinov, M. Weides, and D. P. Pappas, "Concentric transmon qubit featuring fast tunability and an anisotropic magnetic dipole moment," Applied Physics Letters **108** (2016), 10.1063/1.4940230.
[34] A. Blais, R. S. Huang, A. Wallraff, S. M. Girvin, and R. J. Schoelkopf, "Cavity quantum electrodynamics for superconducting electrical circuits: An architecture for quantum computation," Physical Review A - Atomic, Molecular, and Optical Physics **69**, 62320 (2004).
[35] A. Wallraff, D. I. Schuster, A. Blais, L. Frunzio, R.-S. Huang, J. Majer, S. Kumar, S. M. Girvin, and R. J. Schoelkopf, "Strong coupling of a single photon to a superconducting qubit using circuit quantum electrodynamics," Nature **431**, 162–167 (2004).
[36] S. Schlör, J. Lisenfeld, C. Müller, A. Bilmes, A. Schneider, D. P. Pappas, A. V. Ustinov, and M. Weides, "Correlating Decoherence in Transmon Qubits: Low Frequency Noise by Single Fluctuators," Physical Review Letters **123**, 190502 (2019).
[37] J. J. Burnett, A. Bengtsson, M. Scigliuzzo, D. Niepce, M. Kudra, P. Delsing, and J. Bylander, "Decoherence benchmarking of superconducting qubits," npj Quantum Information **5**, 54 (2019).
[38] S. S. Hong, A. T. Papageorge, P. Sivarajah, G. Crossman, N. Didier, A. M. Polloreno, E. A. Sete, S. W. Turkowski, M. P. Da Silva, and B. R. Johnson, "Demonstration of a parametrically activated entangling gate protected from flux noise," Physical Review A **101**, 1–8 (2020).
[39] J. M. Gambetta, C. E. Murray, Y.-K.-K. Fung, D. T. McClure, O. Dial, W. Shanks, J. W. Sleight, and M. Steffen, "Investigating Surface Loss Effects in Superconducting Transmon Qubits," IEEE Transactions on Applied Superconductivity **27**, 1–5.

PLEASE CITE THIS ARTICLE AS DOI: 10.1063/5.0023533